Desalination and Water Treatment
www.deswater.com
doi: 10.5004/dwt.2020.26276

204 (2020) 1–9
November

Daily exergy analysis of passive solar still for maximum yield

Ram Gopal Singh[a,*], G.N. Tiwari[a,b]

[a]*Faculty of Physical Sciences, Shri Ramswaroop Memorial University (SRMU), Lucknow-Dewa Road (UP), India, emails: dr.rgsingh@gmail.com (R.G. Singh), gntiwari@ces.iitd.ernet.in (G.N. Tiwari)*
[b]*Bag Energy Research Society, Sodha Bers Complex, Plot No. 51, Mahamana Nagar, Karaundi, Varanasi, Uttar Pradesh 221005, India*

Received 25 August 2019; Accepted 22 June 2020

ABSTRACT

In the present study, the analysis of the daily exergy of passive solar still is presented. Basically, there are mainly two approaches for the analysis of exergy of solar stills, namely (i) Carnot efficiency and (ii) entropy concept. The daily exergy analysis has been carried out by using both these approaches. It has been found that the daily exergy output based on entropy concept is more acceptable due to the lower value of total known and unknown exergy destruction in comparison with the Carnot method for a given design and climatic parameters. The instantaneous exergy efficiency is also obtained which is found to be in accordance with the results reported by various other studies.

Keywords: Solar still; Exergy analysis; Carnot efficiency; Solar energy

1. Background

The need for potable water for the survival of human beings is well known. There is an acute shortage of fresh drinking water in the remote as well as rural areas of many countries. At many places enough saline water is present but it is not suitable for the drinking and domestic as we as agricultural uses. Advanced desalination systems namely vacuum distillation [1], multi-stage flash distillation [2,3], reverse osmosis [4,5], electrodialysis membrane [6], etc are based on fossil fuel-based grid electricity which is not friendly with environment and climate. In this scenario, the solar distillation method is one of the economical and best ways to have potable water from brackish/hard/saline water [7].

Broadly solar distillation system is classified as the passive and active system and lots of research work have been carried out in the area of passive and active solar distillation [8]. Basically, most of the research work on passive and active solar still has been carried out based on energy conservation to evaluate hourly yield. It is also well known that passive solar distillation operates at a low operating temperature range between 15°C–80°C depending upon climatic conditions [9]. Hence the performance of solar distillation can be carried out based on either first law of thermodynamics (energy conservation) [10,11] or the second law of thermodynamics (exergy analysis). Exergy [12–14] is elucidated as the maximum available work that can be taken out from a system during a process that brings the system into equilibrium with its corresponding environment (i.e., ambient temperature) [14–16]. The specific property of exergy that is in contrast to the energy is that exergy can be destroyed during a process due to irreversibility within the given system during the process [17]. Such an analysis helps to identify which components of the thermal energy system are responsible for irreversibility. So the exergy analysis for the passive solar still with all its components/parts is an effective way to design economically viable solar still [18]. Exergy analysis can be further applied as a powerful thermodynamic technique for estimating and optimizing the performance of energy systems [19].

Gude [14] has used the exergy tool to calculate the thermodynamic efficiency of various desalination processes which are supported by different renewable energy sources.

* Corresponding author.

He identified different processes that contributed to the exergy destruction and also suggested suitable working conditions to mitigate the exergy losses. Vaithilingam and Esakkimuthu [20] have done an energy and exergy analysis of single slope solar still experimentally and found that irrespective of the water depth and in comparison to other components, the highest exergy destruction is observed in the basin liner of the solar still. Mohamed et al. [21] have experimentally observed the role of stone particles placed in solar still over the exergy efficiency. It has been observed that the exergy efficiency of the solar till increases from 65% to 123% when the stone size is doubled from 1 to 2 cm. Recently, Hedayati-Mehdiabadi et al. [22] have studied the exergy performance of basin type double solar still equipped with the phase changed materials and photovoltaic thermal collector on a sample winter and summer days. It has been observed that the exergy efficiency was 48% lower in winter condition than the summer condition. The exergy analysis takes into account the role of ambient temperature, which has a significant effect on the performance of solar stills. It has been seen that many authors have carried out exergy analysis of the solar distillation system by using Carnot efficiency [23–29], which is valid for higher operating temperatures under the second law of thermodynamics as mentioned earlier.

However, the performance of the solar distillation system should be analyzed from daily performance in terms of daily exergy to minimize the daily destruction exergy for maximum yield. There can be two types of destruction exergy, namely known exergy and unknown exergy. Unknown exergy may be due to the presence of heat capacity of condensing cover, absorber plate, internal heat energy generated and quasi-steady-state conditions. It is very difficult to control this unknown exergy, but known exergy can be minimized to have maximum daily exergy output.

Since solar radiation is generated from the sun which is a very high temperature, say about 6,000 K and hence there is not much change in the exergy of solar radiation, therefore, one may consider solar radiation as exergy. However, exergy factor (ψ) for solar radiation coming from the sun has also been derived by Neri et al. [30] which is given as:

$$\psi = \left(1 - \frac{4T_a}{3T_s} - \frac{T_a^4}{3T_s^4}\right) \tag{1}$$

One can see from the above equation that the numerical value for ψ is near to the value 0.94 for any ambient air temperature (T_a) due to the very large value of denominator term (T_s). Even this value will be very close to the value of Carnot efficiency [31]:

$$\eta = \left(1 - \frac{T_a + 273}{6,000}\right) \tag{2}$$

Hence there is no dispute to calculate ψ, either hourly or daily for calculation of the exergy of solar radiation.

Exergy analysis of the solar thermal system, some scientists/researchers have used the concept of Carnot method [31–33] which is valid for higher operating temperature and others have used entropy method [34–36] which is an application to low operating temperature range and hence papers have been published by using both methods. Hence, in this communication, an attempt has been made to develop an expression for the daily exergy for passive solar still which can be applied for the operating temperature of passive solar distillation based on entropy concept (Appendix) to determine unknown destruction which has not been considered earlier.

2. Thermal modeling

For single slope solar still [9], the energy balance of glass cover, water mass, and basin liner can be written as follows.

For glass cover [7]:

$$\alpha_g I(t) + h_1\left(T_w - T_g\right) = h_2\left(T_g - T_a\right) \tag{3}$$

For the water [7]:

$$\alpha_w I(t) + h_3\left(T_b - T_w\right) = m_w C_w \frac{dT_w}{dt} + h_1\left(T_w - T_g\right) \tag{4}$$

For basin [7]:

$$\alpha_b I(t) = h_3\left(T_b - T_w\right) + h_b\left(T_b - T_a\right) \tag{5}$$

Eqs. (3)–(5) will be used to analyze the performance of solar still in terms of water and condensing cover temperature based on the first law of thermodynamics. Numerical computations have been carried out for hourly variation of $I(t)$ and T_a as shown in Fig. 1, the design parameters of Table 1.

With the help of Eqs. (3) and (5), Eq. (4) can be rearranged as:

$$\left(\alpha_w + H\ \alpha_b\right) I(t) = m_w C_w \frac{dT_w}{dt} + U_b\left(T_w - T_a\right) + (h_{\mathrm{rw}} + h_{\mathrm{cw}} + h_{\mathrm{ew}})(T_w - T_g) \tag{6}$$

where $H = h_3/(h_3 + h_b)$, $U_b = h_b h_3/(h_3 + h_b)$, and $h_1 = h_{\mathrm{rw}} + h_{\mathrm{ew}} + h_{\mathrm{cw}}$.

Eq. (6) will be used to analyze the solar still system in terms of exergy. In Eq. (6) the term in the left-hand side (LHS) corresponds to the total energy to the single-slope solar still. On the right-hand side (RHS) the first term corresponds to the energy stored in the water, the second term shows the energy loss from the bottom and the last term corresponds to the energy losses by different heat transfer processes, that is, radiation, convection, and evaporation.

2.1. Thermal analysis

By rearranging the terms in Eq. (3) an expression for glass cover temperature may be calculated as [32]:

$$T_g = \frac{\alpha_g I(t) + h_1 T_w + h_2 T_a}{h_1 + h_2} \tag{7}$$

Also, by using Eqs. (3)–(5) and (7), the differential equation for the water temperature may be derived as [9]:

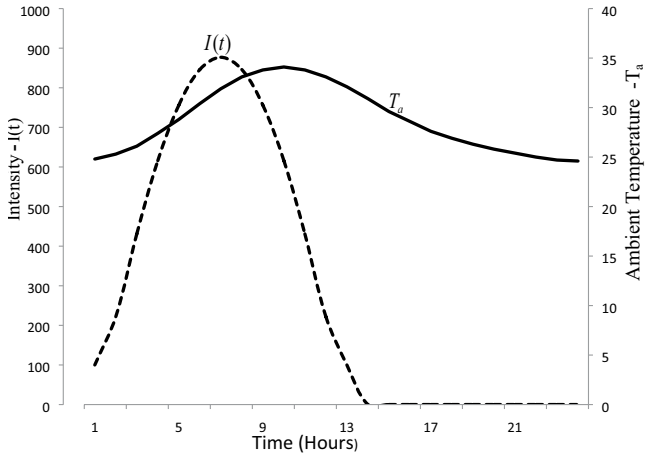

Fig. 1. Variation of solar intensity $I(t)$ and ambient temperature with time.

Table 1
Design parameters for the solar still

Terms	Values
h_3	100 W/m² °C
h_b	1 W/m² °C
α_b	0.50
α_w	0.050
m_w	30–100 kg
d_f	0.1 m

$$\frac{dT_w}{dt} + aT_w = f(t) \tag{8}$$

where $a = U_L/m_wC_w$, $U_L = U_b + U_t$, $U_t = h_1h_2/(h_1 + h_2)$, $f(t) = (\alpha_{eff}I(t) + U_LT_a)/m_wC_w$, and $\alpha_{eff} = \alpha_w + H\alpha_b$.

The solution of Eq. (8) gives the expression for water temperature as [32]:

$$T_w = \left(\frac{\alpha_{\text{eff}}I(t)}{U_L} + T_a\right)\left(1 - e^{at}\right) + T_w e^{-at} \tag{9}$$

2.2. Thermal energy

The rate of thermal energy associated with internal heat transfer processes (radiative, convective, and evaporative) are can be evaluated from Eqs. (7) and (9) as follows:

$$\dot{Q}_{\text{rw}} = h_{\text{rw}}\left(T_w - T_g\right) \tag{9a}$$

$$\dot{Q}_{\text{cw}} = h_{\text{cw}}\left(T_w - T_g\right) \tag{9b}$$

$$\dot{Q}_{\text{ew}} = h_{\text{ew}}\left(T_w - T_g\right) \tag{9c}$$

An instantaneous thermal efficiency can be defined as follows:

$$\eta_i = \frac{h_{\text{ew}}\left(T_w - T_g\right)}{I(t)} \tag{10}$$

2.3. Exergy analysis

The exergy of solar radiation can be computed by using Eq. (1). Further, the exergy of other terms involved in Eq. (6) can be obtained by using two methods as follows:

2.3.1. Using Carnot efficiency (method 1)

In this case, one can use the following expressions:

- For thermal losses from water to glass cover:

$$\psi_1 = 1 - \frac{T_g + 273}{T_w + 273} \tag{11}$$

- For thermal losses from water to ambient:

$$\psi_2 = 1 - \frac{T_a + 273}{T_w + 273} \tag{12}$$

- For final water temperature (T_{wf}) to initial water temperature (T_{wi}):

$$\psi_3 = 1 - \frac{T_{\text{wi}} + 273}{T_{\text{wf}} + 273} \tag{13}$$

where in all the above conversion factors numerator has a lower value than denominators. Further in solar distillation, the variation in operating temperature range is below 20°C–30°C and hence there is not much variation in the numerical value of ψ's. It is also important to note that the numerical value of ψ's will be very small and hence exergy of all term will be very small in numerical values. Most authors have analyzed the solar distillation system by using Eq. (1) for exergy analysis [14–16].

2.3.2. Using the entropy concept (method 2)

In this case, the derivation of exergy expression has been given in the Appendix. For exergy calculation for each term in Eq. (6) the following factors have been used:

- From thermal losses from water to glass cover:

$$\psi_{1d} = \left[1 - \frac{\left(T_a + 273\right)}{\left(T_w - T_g\right)}\ln\frac{T_w + 273}{T_g + 273}\right] \tag{14}$$

- From thermal losses from water to ambient:

$$\psi_{2d} = \left[1 - \frac{\left(T_a + 273\right)}{\left(T_w - T_a\right)}\ln\frac{T_w + 273}{T_a + 273}\right] \tag{15}$$

- From the final water temperature (T_{wf}) to initial water temperature (T_{wi}):

$$\psi_{3d} = \left[1 - \frac{(T_a + 273)}{(T_{\text{wf}} - T_{\text{wi}})} \ln \frac{T_{\text{wf}} + 273}{T_{\text{wi}} + 273}\right] \tag{16}$$

For daily analysis of exergy, with help of the above equations, Eq. (6) can be used to write hourly exergy balance as follows:

$$(\alpha_w + H_2\alpha_b) I(t)\psi = m_w C_w \frac{dT_w}{dt}\psi_3 + U_b(T_w - T_a)\psi_2 + (h_{\text{rw}} + h_{\text{cw}} + h_{\text{ew}})(T_w - T_g)\psi_1 \tag{17}$$

Daily exergy balance can be obtained by summing both sides for the 24 h cycle as follows:

$$\sum_{i=1}^{24}(\alpha_w + H_2\alpha_b) I_i(t)\psi - \sum_{i=1}^{24} h_{\text{ew}_i}(T_{w_i} - T_{g_i})\psi_1 = m_w C_w \sum_{i=1}^{24}\frac{dT_{w_i}}{dt}\psi_3 + \sum_{i=1}^{24} U_b(T_w - T_a)\psi_2 + \sum_{i=1}^{24}(h_{\text{cw}} + h_{\text{ew}})(T_w - T_g)\psi_1 \tag{18}$$

Here $\sum_{i=1}^{24}\frac{dT_{w_i}}{dt} = \frac{(T_{\text{wf}} - T_{\text{wi}})}{3{,}600}$. The numerical values of T_{wf} and T_{wi} will be approximately the same for lower water depth and have no storage effect. However, for larger water depth, T_{wf} will be greater than T_{wi} due to the heat capacity of water (storage effect) and hence the destruction exergy will be always there only for larger water depth. No one has considered this effect of heat capacity to observe the exergy destruction in their previous studies to the best of our knowledge.

The daily exergy for single slope solar still can be evaluated from the following expression:

$$\sum_{i=1}^{24}(\alpha_w + H_2\alpha_b) I_i(t)\psi - \sum_{i=1}^{24} h_{ew_i}(T_{w_i} - T_{g_i})\psi_1 = m_w C_w \frac{(T_{\text{wf}} - T_{\text{wi}})}{3{,}600}\psi_3 + \sum_{i=1}^{24} U_b(T_{w_i} - T_{a_i})\psi_2 + \sum_{i=1}^{24}(h_{\text{cw}_i} + h_{\text{rw}_i})(T_{w_i} - T_{g_i})\psi_1 \tag{19}$$

Eq. (18) can be rewritten in terms of input exergy (Ex_{in}), out exergy (Ex_{out}), known as exergy destruction ($\text{Ex}_{d,k}$) and unknown exergy destruction ($\text{Ex}_{d,\text{uk}}$) which has not been considered earlier, as follows:

$$\text{Ex}_{\text{in}} - \text{Ex}_{\text{out}} = \text{Ex}_{\text{des}} \tag{20}$$

where $\text{Ex}_{\text{des}} = \text{Ex}_{d,k} + \text{Ex}_{d,\text{uk}}$.

$$\text{Ex}_{\text{in}} = \sum_{i=1}^{24}(\alpha_w + H_2\alpha_b) I_i(t)\psi,\ \text{Ex}_{\text{out}} = \sum_{i=1}^{24} h_{\text{ew}_i}(T_{w_i} - T_{g_i})\psi_1$$

$$\text{Ex}_{d,k} = m_w C_w \frac{(T_{\text{wf}} - T_{\text{wi}})}{3{,}600}\psi_3 + \sum_{i=1}^{24} U_b(T_{w_i} - T_{a_i})\psi_2 + \sum_{i=1}^{24}(h_{\text{cw}_i} + h_{\text{rw}_i})(T_{w_i} - T_{g_i})\psi_1$$

$$\text{Ex}_{d,uk} = \text{Ex}_{d-s} + \text{Ex}_{d-b} + \text{Ex}_{d-u}$$

where $\text{Ex}_{d-s} = m_w C_w \frac{(T_{\text{wf}} - T_{\text{wi}})}{3{,}600}\psi_3$, $\text{Ex}_{d-b} = \sum_{i=1}^{24} U_b(T_{w_i} - T_{a_i})\psi_2$

$$\text{Ex}_{d-u} = \sum_{i=1}^{24}(h_{cw_i} + h_{rw_i})(T_{w_i} - T_{g_i})\psi_1 = \text{Ex}_{d-\text{con}} + \text{Ex}_{d-\text{rad}}$$

Eq. (20) is a complete exergy balance equation used in the first method where the values of converging factors ψ_1, ψ_2 and ψ_3 can be obtained from Eqs. (11)–(13). Whereas the exergy balance equation for the second method can be obtained by replacing these ψ's expressions with Eqs. (14)–(16) respectively and schematically has been shown in Fig. 2.

In Fig. 2, the input and output exergy terms are clearly depicted along with the exergy destruction terms for the basin water of single slope solar still. The exergy destruction namely stored radiation and convection, Fig. 2, is referred to as the known exergy destruction. The unknown exergy destruction is not possible to depict in a diagram but calculated and given in Tables 2a and 2b.

Further, instantaneous exergy efficiency can also be written as follow:

$$\eta_i = \frac{\text{Ex}_{\text{out}}}{\text{Ex}_{\text{in}}} = 1 - \frac{\text{Ex}_{\text{des}}}{\text{Ex}_{\text{in}}} \tag{21}$$

3. Results and discussion

Eqs. (7) and (9) have been used to evaluate the hourly variation of water (T_w) and glass cover temperature (T_g), yield (m_w), various internal heat transfer coefficients (h_{rw}, h_{ew}, h_{cw}) and instantaneous thermal efficiency (η_i) for a given design parameter (Table 1), the thermophysical

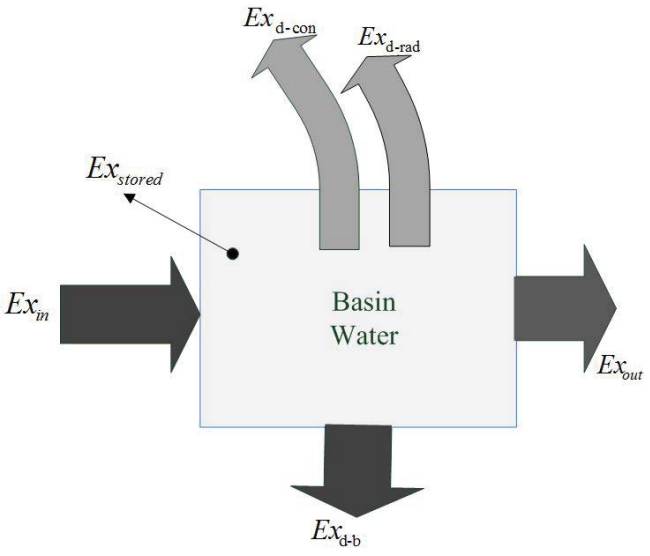

Fig. 2. Daily exergy flow diagram of the solar distillation process referring to Eq. (20).

Table 2a
Daily exergy components for solar still at different water depths by the first method

Water depth (m)	Ex_{in} (kWh)	Ex_{out} (kWh)	Known exergy destruction ($Ex_{d,k}$)					Unknown exergy destruction ($Ex_{d,uk}$) (kWh)	Total exergy destruction (kWh)
			Ex_{store} (kWh)	Ex_{d-b} (kWh)	Ex_{d-rad} (kWh)	Ex_{d-con} (kWh)	$Ex_{d-total}$ (kWh)		
0.03	3,408	19.57	0.42	110.08	7.51	1.95	119.96	3,268.46	3,388.42
0.06	3,408	15.14	25.33	74.89	7.79	2.02	125.17	3,267.69	3,392.86
0.10	3,408	9.92	43.97	47.68	6.42	1.64	109.62	3,288.46	3,398.08

Table 2b
Daily exergy components for solar still at different water depths by the second method

Water depth (m)	Ex_{in} (kWh)	Ex_{out} (kWh)	Known exergy destruction ($Ex_{d,k}$)					Unknown exergy destruction ($Ex_{d,uk}$) (kWh)	Total exergy destruction (kWh)
			Ex_{d-s} (kWh)	Ex_{d-b} (kWh)	Ex_{d-rad} (kWh)	Ex_{d-con} (kWh)	$Ex_{d-total}$ (kWh)		
0.03	3,408	126.82	0.670	56.85	39.82	10.38	107.72	3,173.46	3,281.18
0.06	3,408	68.85	14.18	38.31	32.67	8.47	162.48	3,176.67	3,339.15
0.10	3,408	36.53	23.36	24.27	22.93	5.87	112.96	3,258.51	3,371.47

parameter of vapor (Table 3) and climatic parameters (Fig. 1). The hourly results have been given in Table 4. By using the data of Table 4, it has been observed that the daily numerical value of the LHS term of Eq. (6) is 3,602.13 and that of RHS term is 3,588.47. These results show that there is a deviation of 0.37% which validates the results of energy conservation. This table also shows that the instantaneous thermal efficiency increases with time as expected [33]. Further, it is to be noted that the variation of temperatures of water and glass varies in accordance with solar radiation with a shift in the maximum value of about 3 h due to storage effect in the water of the basin.

Now, we have used Eqs. (11–13) for the first method (Carnot method) and Eqs. (14)–(16). for the second method (entropy method), to evaluate hourly exergy output (yield) and total destruction for an obtained data of Table 4 and the results are shown in Figs. 3a and b, respectively for a water depth of 0.1 m. It is seen that the trends of hourly exergy output in both cases are the same as that of water and glass cover temperatures. However, the trend of exergy destruction is the same as the trends of solar radiation. Further, the hourly exergy by the second method (entropy method) is higher due to minimum destruction as expected (Fig. 3b). Hence we recommend analyzing the exergy analysis of any solar distillation system by using the entropy method only due to its low operating temperature range (much below 100°C), unlike the Carnot method which is valid only for higher operating temperature range (300°C–400°C).

Further, one can see from Fig. 3a that the maximum value of the hourly output exergy for passive single slope solar still is nearly four times higher in the case of method 2 (entropy method) in comparison to method 1 (Carnot method). Again, the maximum hourly total destruction for method 2 (entropy method), Fig. 3b is nearly two times higher than the value evaluated by using method 1 (Carnot method). Here, it is important to mention that hourly exergy input is the same in both methods.

Fig. 4 shows hourly instantaneous exergy efficiency by both methods. It indicates that the variation in hourly exergy obtained by the entropy method is significant due to low operating temperature, unlike the Carnot method. This further justified the accuracy of the second method

Table 3
Thermophysical properties of water vapor

S. No.	Physical quantity	Expression
1	Density (ρ)	$1.299995 - 6.043625 \times 10^{-3} \cdot T + 4.697926 \times 10^{-5} \cdot T^2 - 5.760867 \times 10^{-7} \cdot T^3$
2	Emissivity (∈)	0.82
3	Expansion Factor (β)	$1/(T + 273)$
4	Latent heat of vaporization of water (L)	$2.4935 \times 10^6 \cdot [1-(9.4779 \times 10^{-4} \cdot T + 1.3132 \times 10^{-7}\ T^2 - 4.7974 \times 10^{-9} \cdot T^3)]$
5	Specific heat (C_p)	$1.088022 - 0.010577 \cdot T + 4.769110 \cdot T^2 - 7.898561 \times 10^{-6} \cdot T^3 + 5.122303 \times 10^{-6} \cdot T^4$
6	Stefan-Boltzmann constant (σ)	5.67×10^{-8} W/m^2 K^4
7	Thermal conductivity (K)	$0.024168 + 5.526004 \times 10^{-5} \cdot T + 4.631207 \times 10^{-7} \cdot T^2 - 9.489325 \times 10^{-9} \cdot T^3$
8	Viscosity (μ)	$1.685731 \times 10^{-5} + 9.151853 \times 10^{-8} \cdot T - 2.162762 \times 10^{-9} \cdot T^2 + 3.413922 \times 10^{-11} \cdot T^3$

Table 4
Hourly variations of various temperatures, heat transfer coefficients, yield and thermal efficiency

Time (h)	$I(t)$	T_a (°C)	T_w (°C)	T_g (°C)	h_{cw}	h_{ew}	h_{rw}	$\dot{Q}_{ew}$	$\dot{Q}_{rw}$	$\dot{Q}_{cw}$	$\dot{m}_{ew}$ (kg)	$\eta_{eff\_thermal}$
1	100	24.8	28.870	27.358	1.181	3.188	5.272	4.82	7.97	1.79	0.007	4.8
2	222	25.3	31.395	29.108	1.079	3.082	5.330	7.05	12.19	2.47	0.011	3.2
3	431	26.1	36.536	32.898	1.247	3.962	5.443	14.41	19.80	4.54	0.023	3.3
4	616	27.4	43.532	38.617	1.480	5.843	5.683	28.73	27.93	7.28	0.045	4.7
5	756	28.8	51.362	45.614	1.682	8.952	6.037	51.46	34.70	9.67	0.081	6.8
6	846	30.4	59.126	53.212	1.845	13.676	6.468	80.87	38.25	10.91	0.127	9.6
7	877	31.9	65.947	60.357	1.960	20.121	6.936	112.48	38.77	10.95	0.176	12.8
8	846	33.1	71.090	66.022	2.030	27.638	7.380	139.99	37.38	10.28	0.219	16.5
9	756	33.8	73.996	69.420	2.058	34.565	7.736	158.20	35.41	9.42	0.248	20.9
10	616	34.1	74.402	70.183	2.048	38.758	7.949	163.50	33.53	8.64	0.256	26.5
11	431	33.8	72.122	68.110	2.004	38.752	7.989	155.47	32.05	8.04	0.243	36.1
12	222	33.1	67.340	63.426	1.929	34.384	7.841	134.60	30.70	7.56	0.211	60.6
13	100	32.1	61.736	57.743	1.834	27.245	7.525	108.79	30.05	7.32	0.170	–
14	0	30.9	55.730	51.750	1.763	20.933	7.160	83.32	28.50	7.02	0.130	–
15	0	29.6	50.747	46.703	1.686	15.633	6.785	63.22	27.44	6.82	0.099	–
16	0	28.6	46.603	42.672	1.642	12.285	6.482	48.28	25.48	6.45	0.076	–
17	0	27.6	43.109	39.341	1.589	9.930	6.242	37.41	23.52	5.99	0.059	–
18	0	26.9	40.177	36.662	1.540	8.247	6.046	28.98	21.25	5.41	0.045	–
19	0	26.3	37.702	34.462	1.485	6.986	5.888	22.63	19.07	4.81	0.035	–
20	0	25.8	35.607	32.652	1.431	6.031	5.758	17.82	17.01	4.23	0.028	–
21	0	25.4	33.831	31.163	1.377	5.286	5.651	14.10	15.07	3.67	0.022	–
22	0	25.0	32.310	29.899	1.323	4.693	5.563	11.32	13.41	3.19	0.018	–
23	0	24.7	31.012	28.855	1.273	4.218	5.488	9.10	11.84	2.75	0.014	–
24	0	24.6	29.928	28.050	1.221	3.821	5.426	7.18	10.19	2.29	0.011	–

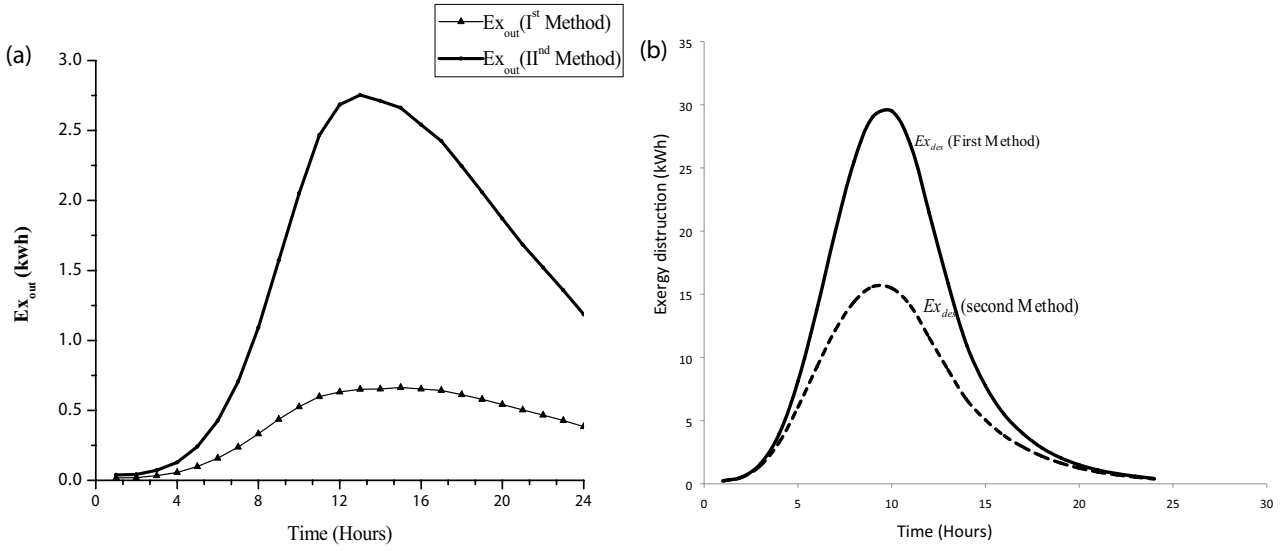

Fig. 3. (a) Hourly variation of output exergy of passive single slope solar still at 0.10 m water depth and (b) hourly variation of total exergy destruction of single slope passive solar still at 0.10 m depth.

(entropy method) in evaluating the exergy analysis of solar distillation in comparison with the first method (Carnot method) [27,34].

Here, it is important to observe that the maximum value of hourly exergy efficiency has been noted as about 8% which is in accordance with the results reported by others [9–11], but by the first method, this value is about 1% which is unrealistic. Further, it can be seen that exergy efficiency is much lower than thermal efficiency (Table 3) as per our expectations.

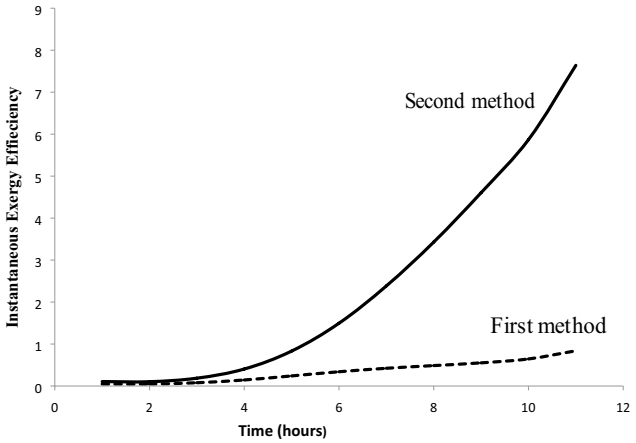

Fig. 4. The hourly instantaneous exergy efficiency of passive solar still.

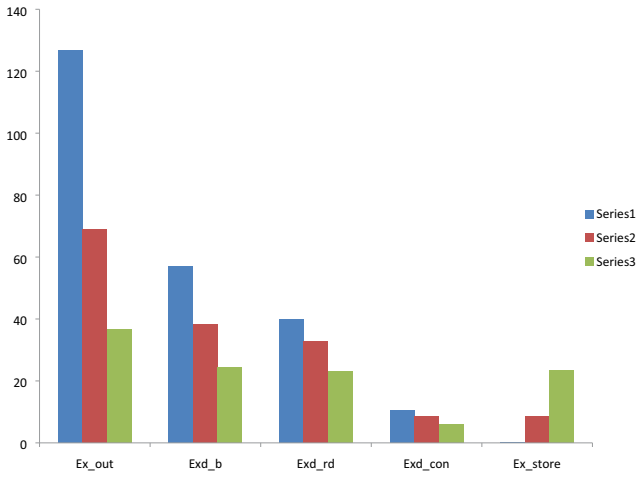

Fig. 5. Daily exergy in kWh for different water depths in passive single slope solar still, by the second method [series 1 (0.03 m), series 2 (0.06 m) and series 3 (0.10 m)].

Effect of water depth on daily exergy values for the passive single slope solar stills computed by first and second methods respectively are given in Tables 2a and 2b respectively. It can be seen that the exergy input is the same in all conditions but the daily output exergy, known exergy destruction and unknown exergy destruction are different at different water depths. As per our conclusion, we have also computed exergy at different component of passive single slope solar still namely exergy output (evaporation), basin liner, radiation, convection and stored and the results have been summarized in Fig. 5.

From this figure and Table 4, one can conclude that the exergy output decreases and stored exergy destruction increase with an increase of water depth as expected. This effect has not been considered by any other studies. The unknown destruction for any water depth in the basin of the single-slope solar still can be easily evaluated from the proposed model which has also not been considered by any earlier studies.

4. Conclusions

Based on the present studies, the following conclusions have been drawn:

- Exergy analysis of passive solar single solar still should be analyzed by the entropy method due to minimum total exergy destruction, Fig. 3 due to its low operating temperature range.
- Unknown exergy destruction is marginally lower in the case of the second method (entropy method) as per expectation. The known destruction decreases with the decrease of water depth (Fig. 5) due to the storage effect of water in the basin of solar still.
- There is a 71% decrease in exergy out for varying water depth from 0.03 to 0.06 m which is in accordance with the result reported by various authors [15,18].
- Exergy destruction decreases by the basin (57%), radiation (42%) and convection (43%) with an increase in water depth. However, the stored exergy destruction is increased by as expected due to an increase in the thermal capacity of water mass, Fig. 5.
- Exergy analysis of the solar distillation system should be analyzed by using the second method based on the entropy concept.

Symbols

C_p — Specific heat capacity, J/kg K
Ex_{in} — Input exergy
Ex_{out} — Output exergy
Ex_d — Distruction exergy
Ex_{d-s} — Distruction exergy stored
$Ex_{d,k}$ — Known exergy destruction
$Ex_{d,uk}$ — Unknown exergy destruction
Ex_{d-d} (Ex_{d-b}) — Distruction exergy to the downward direction, basin
Ex_{d-con} — Distruction exergy to conduction
Ex_{d-rad} — Distruction exergy to radiation
Ex_{d-u} — Distruction exergy to the upward direction
G_r — Grashof number
g — Gravitational acceleration, m/s^2
h_1 — Total internal heat transfer coefficient, W/m^2 °C
h_2 — Heat transfer coefficient from glass to ambient, W/m^2 °C
h_3 — Heat transfer coefficient from basin to water, W/m^2 °C
h_{cw} — Convective heat transfer coefficient from the water surface to glass cover, W/m^2 °C
h_{ew} — Evaporative heat transfer coefficient from the water surface to glass cover, W/m^2 °C
h_{rw} — Evaporative heat transfer coefficient from the water surface to glass cover, W/m^2 °C
I_T — Solar irradiance, W/m
K_v — Thermal conductivity of humid air W/m °C
K_f — Thermal conductivity of humid air, W/mK
L — Latent heat, J/kg
$\dot{m}_{ew}$ — Distillate output from still, kg
Nu — Nusselt number
Pr — Prandtl number

P_{wo} — Partial vapor pressure at water surface, Pa
P_{go} — Partial vapor pressure at water surface, Pa
$\dot{Q}_{ew}$ — Rate of evaporative heat transfer, W/m²
$\dot{Q}_{cw}$ — Rate of evaporative heat transfer, W/m²
$\dot{Q}_{rg}$ — Rate of radiative heat transfer from the condensing surface to the atmosphere, W/m²
$\dot{Q}_{cg}$ — Rate of convective heat transfer from the condensing surface to ambient air, W/m²
T_s — Tempertaure of sun, °C
T_{wi} — Initial water temperature, °C
T_{wo} — Initial temperature of water, °C
T_{go} — Initial temperature of glass cover, °C
U_b — Bottom heat loss coefficient, W/m² °C
U_t — Top heat loss coefficient from water surface to ambient, W/m² °C
U_L — Overall heat transfer coefficient, W/m² °C
V — Wind velocity, m/s

Greek letters

α_b — Absorptivity of the basin
α_w — Absorptivity of the water
β — Coefficient of volumetric expansion coefficient, 1/K
ρ — Density, kg/m³
μ — Viscosity, N s/m²
ψ — Exergy factor
η — Carnot efficiency
η_i — Instantaneous thermal efficiency
η_{iex} — Instantaneous exergy efficiency

References

[1] G.Z. Zha, C.F. Yang, Y.K. Wang, X.Y. Guo, W.L. Jiang, B. Yang, New vacuum distillation technology for separating and recovering valuable metals from a high value-added waste, Sep. Purif. Technol., 209 (2019) 863–869.
[2] R.S. Silver, Multi-stage flash distillation. The first 10 years, Desalination, 9 (1971) 3–17.
[3] O.A. Hamed, M.Ak. Al-Sofi, M. Imam, G.M. Mustafa, K. Bamardouf, H. Al-Washmi, Simulation of multistage flash desalination process, Desalination, 134 (2001) 195–203.
[4] I.G. Wenten, Khoiruddin, Reverse osmosis applications: prospect and challenges, Desalination, 391 (2016) 112–125.
[5] K.H. Park, J.B. Kim, D.R. Yang, S.W. Hong, Towards a low-energy seawater reverse osmosis desalination plant: a review and theoretical analysis for future directions, J. Membr. Sci., 595 (2020) 117607, https://doi.org/10.1016/j.memsci.2019.117607.
[6] Y. Tanaka, Ion Exchange Membranes: Fundamentals and Applications, 2nd ed., Elsevier B.V., Amsterdam, 2015.
[7] G.N. Tiwari, L. Sahota, Advanced Solar-Distillation Systems: Basic Principles, Thermal Modeling, and Its Application, 1st ed., Springer, Singapore, 2017.
[8] R. Balan, J. Chandrasekaran, S. Shanmugan, B. Janarthanan, S. Kumar, Review on passive solar distillation, Desal. Water Treat., 28 (2011) 217–238.
[9] G.N. Tiwari, A. Tiwari, Shyam, Handbook of Solar Energy: Theory, Analysis and Applications, Springer, Singapore, 2016.
[10] H.K. Jani, K.V. Modi, A review on numerous means of enhancing heat transfer rate in solar-thermal based desalination devices, Renewable Sustainable Energy Rev., 93 (2018) 302–317.
[11] H.K. Jani, K.V. Modi, Experimental performance evaluation of single basin dual slope solar still with circular and square cross-sectional hollow fins, Sol. Energy, 179 (2019) 186–194.
[12] H.U. Helvacı, G.G. Akkurt, Thermodynamic Performance Evaluation of a Geothermal Drying System, I. Dincer, A. Midilli, H. Kucuk, Eds., Progress in Exergy, Energy, and the Environment, Springer, Cham, 2014.
[13] J. Szargut, Exergy Method: Technical and Ecological Applications: Technical and Ecological Applications, International Series on Developments in Heat Transfer, Vol. 18, WIT Press, United Kingdom, 2005, p. 164.
[14] V.G. Gude, Use of exergy tools in renewable energy driven desalination systems, Therm. Sci. Eng. Progr., 8 (2018) 154–170.
[15] V.G. Gude, N. Nirmalakhandan, Desalination using low-grade heat sources, J. Energy Eng., 134 (2008) 95–101.
[16] V.G. Gude, N. Nirmalakhandan, S. Deng, A. Maganti, Desalination at low temperatures: an exergy analysis, Desal. Water Treat., 40 (2018) 272–281.
[17] K.R. Ranjan, S.C. Kaushik, Energy, exergy and thermo-economic analysis of solar distillation systems: a review, Renewable Sustainable Energy Rev., 27 (2013) 709–723.
[18] R. Kant, O. Prakash, R. Tripathi, A. Kumar, Exergy Analysis of Active and Passive Solar Still, A. Kumar, O. Prakash, Eds., Solar Desalination Technology, 1st ed., Springer Nature, Singapore, 2019, pp. 261–273.
[19] A. Bejan, Advanced Engineering Thermodynamics, 4th ed., John Wiley & Sons Inc., New Jersey, 2016.
[20] S. Vaithilingam, G.S. Esakkimuthu, Energy and exergy analysis of single slope passive solar still: an experimental investigation, Desal. Water Treat., 55 (2015) 1433–1444.
[21] A.F. Mohamed, A.A. Hegazi, G.I. Sultan, E.M.S. El-Said, Augmented heat and mass transfer effect on performance of a solar still using porous absorber: experimental investigation and exergetic analysis, Appl. Therm. Eng., 150 (2019) 1206–1215.
[22] E. Hedayati-Mehdiabadi, F. Sarhaddi, F. Sobhnamayan, Exergy performance evaluation of a basin-type double-slope solar still equipped with phase-change material and PV/T collector, Renewable Energy, 145 (2020) 2409–2425.
[23] H. Aghaei Zoori, F. Farshchi Tabrizi, F. Sarhaddi, F. Heshmatnezhad, Comparison between energy and exergy efficiencies in a weir type cascade solar still, Desalination, 325 (2013) 113–121.
[24] S. Nazari, H. Safarzadeh, M. Bahiraei, Experimental and analytical investigations of productivity, energy and exergy efficiency of a single slope solar still enhanced with thermoelectric channel and nanofluid, Renewable Energy, 135 (2019) 729–744.
[25] S.W. Sharshir, A.H. Elsheikh, G.L. Peng, N. Yang, M.O.A. El-Samadony, A.E. Kabeel, Thermal performance and exergy analysis of solar stills – a review, Renewable Sustainable Energy Rev., 73 (2017) 521–544.
[26] S.W. Sharshir, G.L. Peng, A.H. Elsheikh, E.M.A. Edreis, M.A. Eltawil, T. Abdelhamid, A.E. Kabeel, J.F. Zang, N. Yang, Energy and exergy analysis of solar stills with micro/nano particles: a comparative study, Energy Convers. Manage., 177 (2018) 363–375.
[27] E. Shanazari, R. Kalbasi, Improving performance of an inverted absorber multi-effect solar still by applying exergy analysis, Appl. Therm. Eng., 143 (2018) 1–10.
[28] M.S. Yousef, H. Hassan, Assessment of different passive solar stills via exergoeconomic, exergoenvironmental, and exergoenviroeconomic approaches: a comparative study, Sol. Energy, 182 (2019) 316–331.
[29] A.L.S. Chávez, H. Terres, A. Lizardi, R. López, Preface: international conference on recent trends in physics (ICRTP 2016), J. Phys. Conf. Ser., 729 (2017) 012009.
[30] M. Neri, D. Luscietti, M. Pilotelli, Computing the exergy of solar radiation from real radiation data, J. Energy Resour. Technol., 139 (2017) 061201.
[31] M.J. Moran, H.N. Shapiro, D.D. Boettner, M.B. Bailey, Fundamentals of Engineering Thermodynamics, 9th ed., Wiley, USA, 2018.
[32] G.N. Tiwari, Solar Energy: Fundamentals, Design, Modelling and Application, Narosa Publication, New Delhi, India, 2002.
[33] R.G. Singh, G.N. Tiwari, Simulation performance of single slope solar still by using iteration method for convective heat transfer coefficient, Groundwater Sustainable Dev., 10 (2020) 100287.

[34] J.C. Torchia-Núñez, M.A. Porta-Gándara, J.G. Cervantes-de Gortari, Exergy analysis of a passive solar still, Renewable Energy, 33 (2008) 608–616.
[35] A. Layek, Exergetic analysis of basin type solar still, Eng. Sci. Technol. Int. J., 21 (2018) 99–106.
[36] S.M. Elshamy, E.M.S. El-Said, Comparative study based on thermal, exergetic and economic analyses of a tubular solar still with semi-circular corrugated absorber, J. Cleaner Prod., 195 (2018) 328–339.

Appendix

A1. Derivation of exergy of thermal energy based on entropy concept

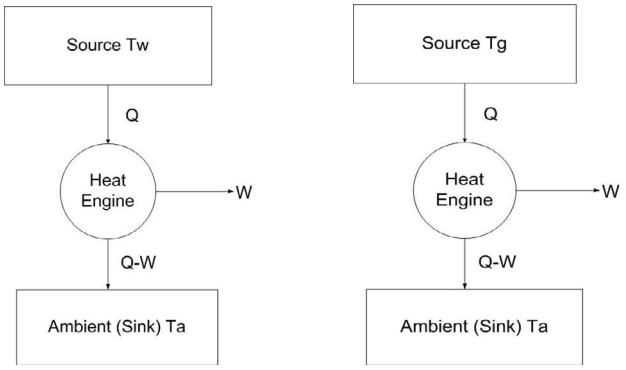

(a) (b)

Fig. A1. Block diagram for determining the maximum work done by using the concept of entropy.

Referring to Fig. A1a, the entropy of water heat engine and ambient can be written as follows:

$$\left(\Delta S\right)_{\text{water}} = \int_{T_w}^{T_a} \frac{C_p dT}{T_w} = C_p \ln \frac{T_a}{T_w} \tag{A1}$$

$$\left(\Delta S\right)_{\text{heat engine}} = 0 \tag{A2}$$

$$\left(\Delta S\right)_{\text{ambient}} = \frac{Q-W}{T_a} \tag{A3}$$

The total entropy of a system, Fig. 1a can be written as follows:

$$\left(\Delta S\right)_{\text{total}} = \left(\Delta S\right)_{\text{water}} + \left(\Delta S\right)_{\text{heat engine}} + \left(\Delta S\right)_{\text{ambient}} = C_p \ln \frac{T_a}{T_w} + \frac{Q-W}{T_a} \tag{A4}$$

Eq. (4) can be referred to as universe entropy as:

$$\left(\Delta S\right)_{\text{universe}} = C_p \ln \frac{T_a}{T_w} + \frac{Q-W}{T_a} \tag{A5}$$

By entropy principle, $(\Delta S)_{\text{universe}} \geq 0$, hence Eq. (A5) becomes as:

$$C_p \ln \frac{T_a}{T_w} + \frac{Q-W}{T_a} \geq 0$$

or,

$$W \leq Q + T_a C_p \ln \frac{T_a}{T_w} \tag{A6}$$

From the above equation, maximum work between water and ambient becomes as:

$$W_{\text{max},1} = C_p \left[\left(T_w - T_a\right) + T_a \ln \frac{T_a}{T_w} \right] \tag{A7}$$

Similarly, in Fig. A1b, W_{max} between glass and ambient can be written as:

$$W_{\text{max},2} = C_p \left[\left(T_g - T_a\right) + T_a \ln \frac{T_a}{T_g} \right] \tag{A8}$$

By using Eqs. (A7) and (A8), maximum work between water and glass (condensing cover) can be written as:

$$W_{\text{max}} = W_{\text{max},1} - W_{\text{max},2} = C_p \left[\left(T_w - T_g\right) - T_a \ln \frac{T_w}{T_g} \right] \tag{A9}$$

The above maximum work is nothing but exergy, hence exergy of a system is given by:

$$E_{x,wg} = C_p \left[\left(T_w - T_g\right) - T_a \ln \frac{T_w}{T_g} \right] \tag{A10}$$

Since $\dot{m}C_p = hA$, (W/°C) hence exergy in terms of heat transfer coefficient (h) becomes:

$$E_{x,wg} = h \left[\left(T_w - T_g\right) - T_a \ln \frac{T_w}{T_g} \right] \tag{A11}$$

It is important to mention that all temperature values are considered in Kelvin. Further, $C_p = C_w$ is the same for both Figs. 1a and b due to condensed water at the inner surface of condensing cover.